Science Advances

AAAS

advances.sciencemag.org/cgi/content/full/4/4/eaas8667/DC1

Supplementary Materials for

A low-barrier hydrogen bond mediates antibiotic resistance in a noncanonical catalytic triad

Prashasti Kumar, Engin H. Serpersu, Matthew J. Cuneo

Published 4 April 2018, *Sci. Adv.* **4**, eaas8667 (2018)
DOI: 10.1126/sciadv.aas8667

This PDF file includes:

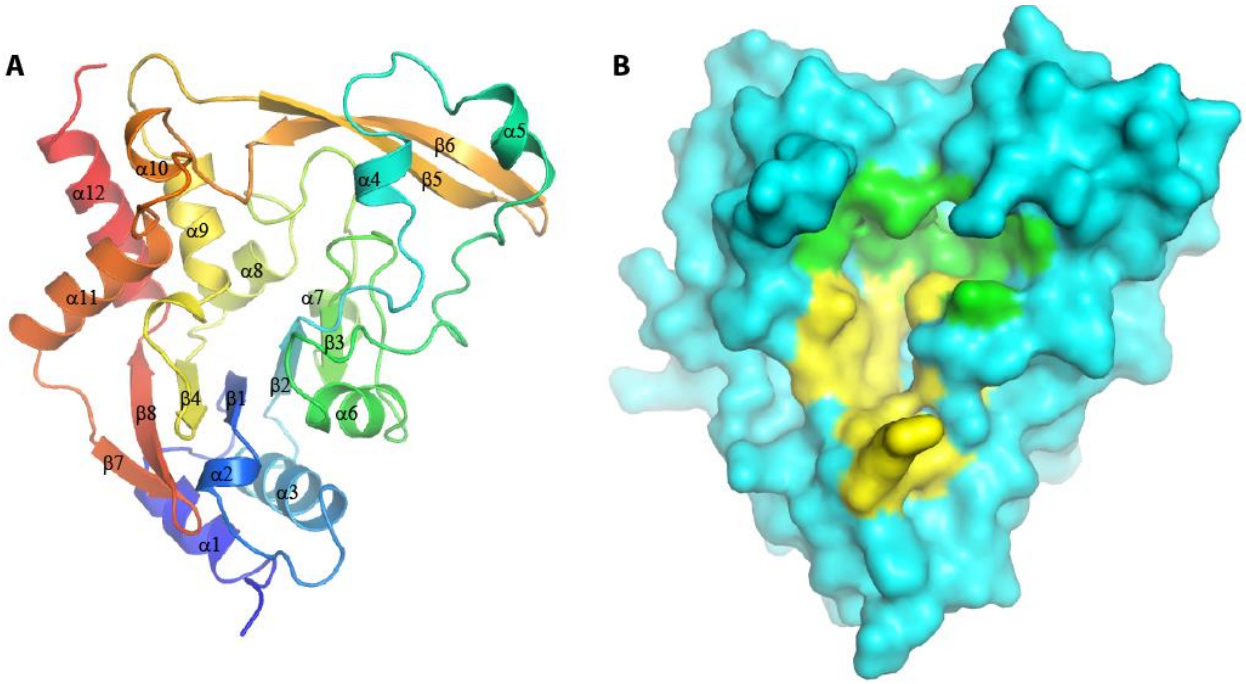

fig. S1. Overall structure of apo acetyltransferase AAC-VIa. (**A**) Ribbon representation of AAC-VIa with ordering of secondary structure elements indicated from N– to C–terminus. (**B**) Surface representation of apo AAC-VIa. Two large cavities present in the apo AAC-VIa are indicated by green and yellow surfaces.

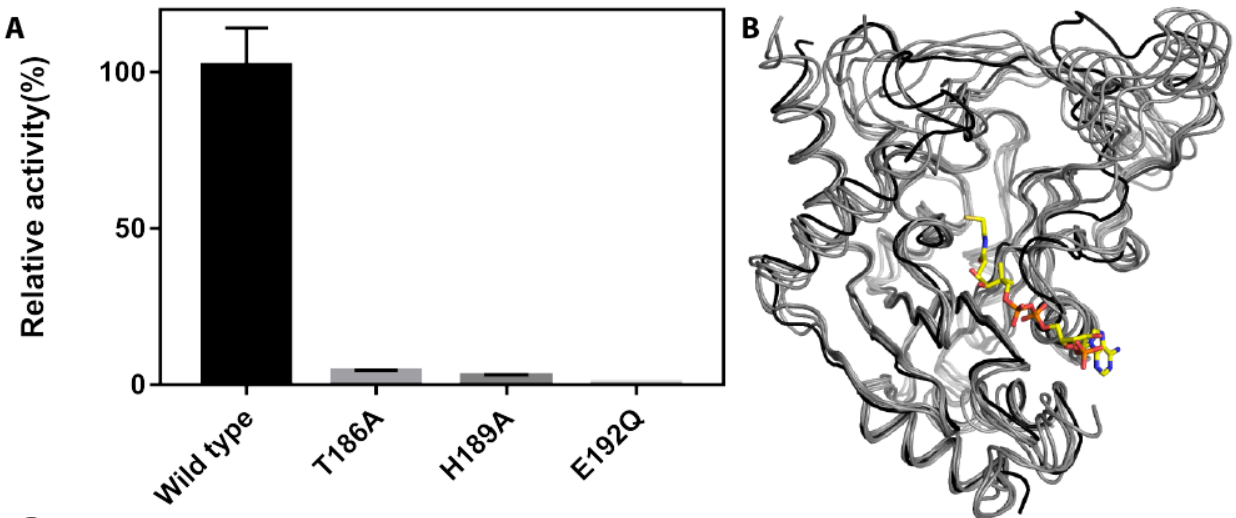

C

```
3E4F      --------NDIVASTQLPN---TIKTITNDLRKLGLKKGMTVIVHSSLSSIGWISGGAVA 50
2NYG      ------SLKKIVESTTFPR---TKQSITEDLKALGLKKGMTVLVHSSLSSIGWVNGGAVA 51
3SMA      MIRHIDARREDLEPDRQDRELVTRDRLASDLAALGVRPGGVLLVHASLSALGWVCGGAQA 60
5HT0      ----------------MSSRVSTRSSLAEDLRAIGLADGDAVLVHAALRKVGKIVGGPDD 44
AAC-IIIb  -------------MTSATASFATRTSLAADLAALGLAWGDAIMVHAAVSRVGRLLDGPDT 46
AAC-VIa   -MTDPRKNGDLHEPATAPATPWSKSELVRQLRDLGVRSGDMVMPHVSLRAVGPLADGPQT 59
                                :   :. :*  :*:  *  :: * ::  :* : .*.
3E4F      VVEALMEVITEEGTIIMPTQSSDLSDPKHWSRPPVPEEWWQIIRDNVPAFEPHITP-TRA 109
2NYG      VIQALIDVVTEEGTIVMPSQSVELSDPKEWGNPPVPEEWWDIIRESMPAYNSNYTPTTRG 111
3SMA      VVLALQDAVGKEGTLVMPTFSGDLSDPSTWRRPPVPEDWWPVIREQMPPFDPDLTP-TRG 119
5HT0      ILDAMRDVIGPAGTVLGYADWQ----LEDEIRDD------PAMREHIPAFDPLRSRSIRD 94
AAC-IIIb  IIAALRDTVGPGGTVLAYADWE----ARYEDLVDDAGRVPPEWREHVPPFDPQRSRAIRD 103
AAC-VIa   LVDALIEAVGPTGNILAFVSWR----DSPYEQTLGHDAPPAAIAQSWPAFDPDHAPAYPG 115
           :: *: :.:   *.::                              :  *.::.  :
3E4F      MGKVVECFRTYPNVVRSNHPLGSFAAWGRHAEEITVNQSLSMSLGEESPLRKIYDLDGYI 169
2NYG      MGQIVELFRSYPEVKRSNHPNYSFVAWGKHKNKILNQHPLEFGLGEQSPLGKLYIRESYV 171
3SMA      MGAVAECFRRAAGAVRSGHPQNSFAAWGAHAEQVVAEHGLTERLGRGSPLEQVYRLDGQV 179
5HT0      NGFWPELIRTTPGALRSASPGASMAAIGGEAEWFTADHALDYGYGPRSPLGKLVEAKGKV 154
AAC-IIIb  NGVLPEFLRTTPGTLRSGNPGASLVALGAKAEWFTADHPLDYGYGEGSPLAKLVEAGGKV 163
AAC-VIa   FGAINEFIRTYPGCRRTAHPDASMAAIGPDAAWLVAPHEMGAAYGPRSPIARFLAHAGKI 175
           *   * :*  .   *:  *  *:.* * .   .   : :    *  **: :.    . :
3E4F      LLIGVGYDSNTSVHLSEVR--SGACELIKVGAPIIENGERVWKEFVDMDYD--------- 218
2NYG      LLLGADFDSSTCFHLAEYR--IPYQKIINRGAPIIVEGKRVWKEYKELEFR--------- 220
3SMA      LLLGCGFESNTSFHLAEYRTAYPGRRSHRRRVPVPEGDRVRWVEQEDIVYF--------- 230
5HT0      LMLGAPLDTMTLLHHAEHLADFPNKRILRYEAPILVDGEKVWRWFEEFDTS---DPPDG- 210
AAC-IIIb  LMLGAPLDTLTLLHHAEHLADIPGKRIKRIEVPFATPTGTQWRMIEEFDTG---DPIVAG 220
AAC-VIa   LSIGAGPDAVTALHYAEAVARIEGKRRVTYSMPLLREGKRVWVTTSDWDSNGILDEYAAP 235
          * :*   :: * .* :*        .      *.       *    :
3E4F      --SDKFVEIGVEFEQKGT-VTMGKIGNAKCRLMKQRDIVDFGTEWFRKKN---------- 265
2NYG      --EELFQEVGQAFEAEHN-MKVGKVGSANCRLFSLTEAVDFAEKWFINNDSKNIKK---- 273
3SMA      --EEDFQTMGESCLTRTPGHSRGTVGEAAAVLYGQRAFVDLACEWMTAHRDLARAVGA-- 286
5HT0      LADDYFAGIVEEFLATGR-GKRGKIGEASSVLVPADEIVAFAVDWLERWGRTAR------ 263
AAC-IIIb  LAEDYFAGIVTEFLASGQ-GRQGLIGAAPSVLVDAAAITAFGVTWLEKRFGTPSP----- 274
AAC-VIa   DGPDAVERIARDYLARTR-VAQGPVGGAQSRLIDAADIVSFGIEWLEARHAAPAAAALKP 294
             : .  :             * :* * . *      . :.  *:
```

fig. S2. Kinetics and homologs of AAC-VIa. (**A**) Steady state kinetics of AAC–VIa and the three active site mutants. (**B**) Structural superimposition of closest AAC–VIa structural homologs identified by the DALI server. (**C**) Sequence alignment of AAC–VIa structural homologs. The active site catalytic triad in AAC-VIa is highlighted in magenta, antibiotic binding site residues in green and acetyl–CoA binding residues in orange.

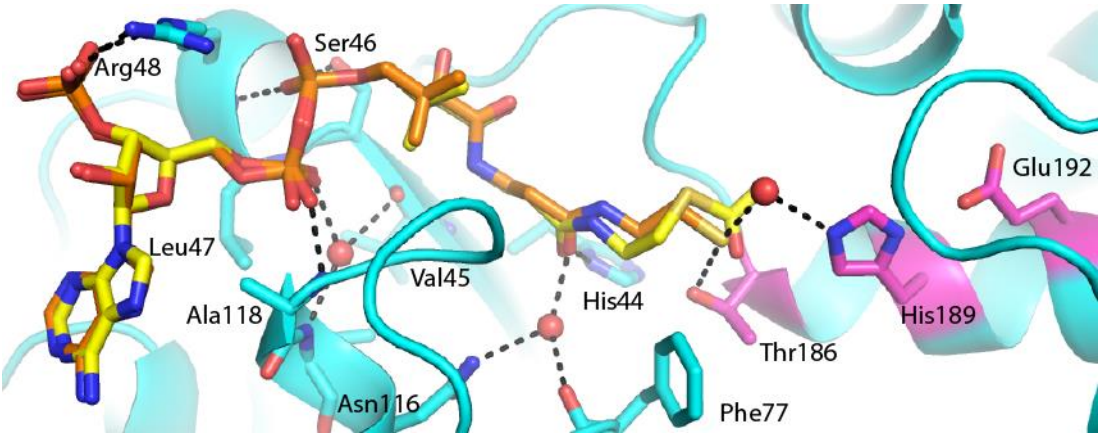

fig. S3. The binary AAC-VIa–CoASH complex. Close–up view of CoASH (orange carbon atoms) interaction with AAC-VIa. The CoASH is superimposed with the acetyl-CoA (yellow carbon atoms) from the binary enzyme–acetyl-CoA structure. Hydrogen bonds are represented as black dashed lines and water molecules are shown as red spheres. The active site resides have carbon atoms colored magenta.

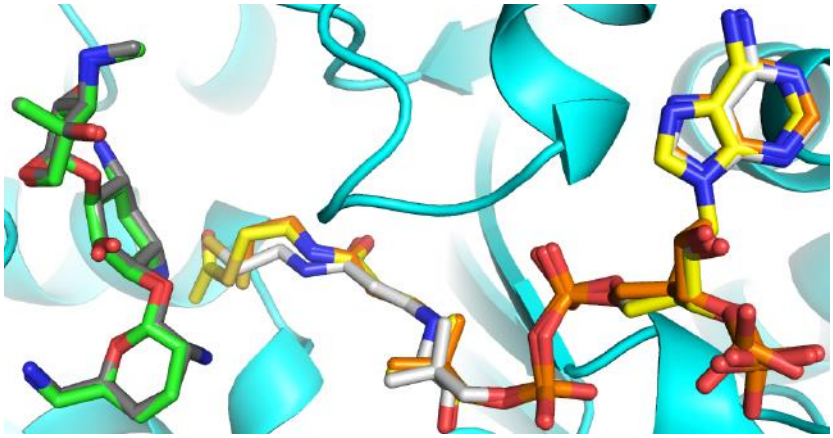

fig. S4. Overlay of ternary enzyme-CoASH-sisomicin complex with binary complexes of the enzyme with CoASH, acetyl-CoA, and sisomicin. The ligands of the ternary enzyme–CoASH–sisomicin (orange/green carbon atoms) complex are found in the same conformation as in the binary enzyme–sisomicin (dark grey carbon atoms) and enzyme–acetyl-CoA (yellow carbon atoms) complexes. The pantetheine tail of the CoASH in the binary enzyme–CoASH (light grey carbon atoms) is found in a different conformation than the CoASH in the binary and ternary complexes.

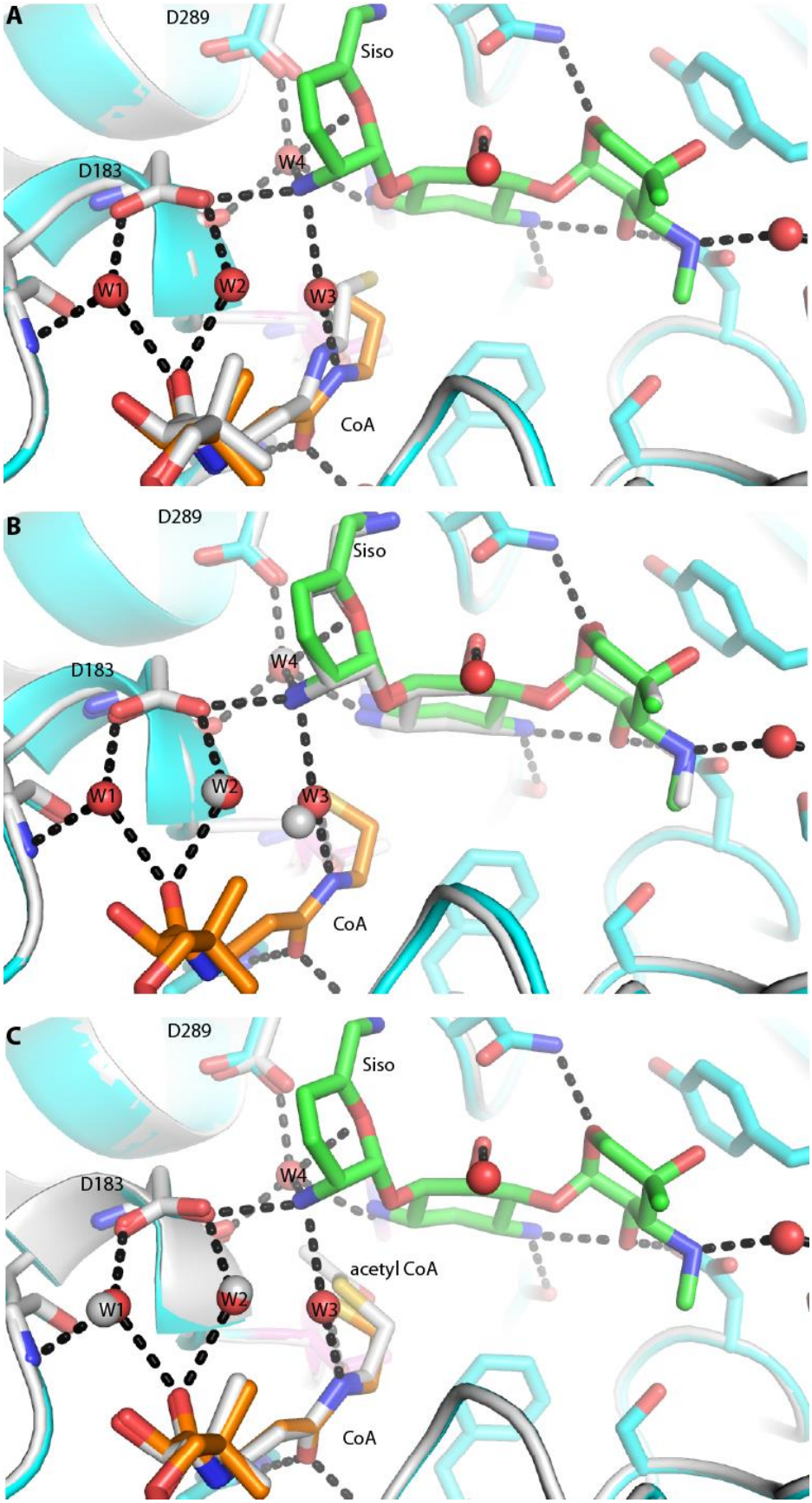
A
D289
Siso
D183
W4
W1
W2
W3
CoA
B
D289
Siso
D183
W4
W1
W2
W3
CoA
C
D289
Siso
D183
W4
acetyl CoA
W1
W2
W3
CoA

fig. S5. Sisomicin-mediated ordering of acetyl-CoA binding site. (**A**) Superposition of the structures of the binary enzyme–CoASH complex (grey carbon atoms) with the ternary enzyme–CoASH–sisomicin complex (cyan protein carbon atoms, with sisomicin carbon atoms colored green and CoASH carbon atoms colored orange). Substrate waters 1–4 are absent in the binary complex. (**B**) Superposition of the enzyme–sisomicin (grey carbon atoms) structure with the ternary enzyme–CoASH–sisomicin complex (cyan protein carbon atoms, with sisomicin carbon atoms colored green and CoASH carbon atoms colored orange). Substrate waters 2–4 are present in the binary complex. (**C**) Superposition of the enzyme–acetyl-CoA binary (grey carbon atoms) structure with the ternary enzyme–CoASH–sisomicin complex (cyan protein carbon atoms, with sisomicin carbon atoms colored green and CoASH carbon atoms colored orange) structure. Substrate waters 1 and 2 are present in the binary complex.